

## Research



**Cite this article:** Feng B-F, Ling L, Zhu Z. 2021

A focusing and defocusing semi-discrete complex short-pulse equation and its various soliton solutions. *Proc. R. Soc. A* **477**: 20200853. <https://doi.org/10.1098/rspa.2020.0853>

Received: 25 October 2020

Accepted: 3 February 2021

**Subject Areas:**

mathematical physics, applied mathematics

**Keywords:**

generalized Darboux transformation, semi-discrete complex short-pulse equation, bright and dark soliton, breather, rogue wave

**Author for correspondence:**

Liming Ling

e-mail: [linglm@scut.edu.cn](mailto:linglm@scut.edu.cn)

# A focusing and defocusing semi-discrete complex short-pulse equation and its various soliton solutions

Bao-Feng Feng<sup>1</sup>, Liming Ling<sup>2</sup> and Zuonong Zhu<sup>3</sup>

<sup>1</sup>School of Mathematical and Statistical Sciences, The University of Texas Rio Grande Valley Edinburg, Edinburg, TX 78541-2999, USA

<sup>2</sup>School of Mathematics, South China University of Technology, Guangzhou 510640, People's Republic of China

<sup>3</sup>School of Mathematical Sciences, Shanghai Jiaotong University, Shanghai 200240, People's Republic of China

B-FF, 0000-0002-2529-897X; LL, 0000-0002-3051-4366; ZZ, 0000-0001-6369-7552

In this paper, we are concerned with a semi-discrete complex short-pulse (sdCSP) equation of both focusing and defocusing types, which can be viewed as an analogue to the Ablowitz–Ladik lattice in the ultra-short-pulse regime. By using a generalized Darboux transformation method, various soliton solutions to this newly integrable semi-discrete equation are studied with both zero and non-zero boundary conditions. To be specific, for the focusing sdCSP equation, the multi-bright solution (zero boundary conditions), multi-breather and high-order rogue wave solutions (non-zero boundary conditions) are derived, while for the defocusing sdCSP equation with non-zero boundary conditions, the multi-dark soliton solution is constructed. We further show that, in the continuous limit, all the solutions obtained converge to the ones for its original CSP equation (Ling *et al.* 2016 *Physica D* **327**, 13–29 (doi:10.1016/j.physd.2016.03.012); Feng *et al.* 2016 *Phys. Rev. E* **93**, 052227 (doi:10.1103/PhysRevE.93.052227)).

## 1. Introduction

Optics and photonics are key enabling technologies that impact society in a multitude of areas, including information and communications, imaging and sensing, healthcare, energy, manufacturing and national security.

Building upon impressive progress in fundamental optical science and in nanotechnology in recent years, optics and photonics have become drivers for technological innovation and economic growth. The most recent advances in nonlinear optics include the generation and applications of ultra-short optical pulses, whose time duration is from the order of femtoseconds ( $10^{-15}$ ) to the order of attoseconds ( $10^{-18}$ ), which led to the Nobel Prize in Chemistry in 1999 [1] and the Nobel Prize in Physics in 2018 [2]. It is an important topic to study the mathematical models of optical pulse propagation in nonlinear media [3–5]. When the range of short-pulse widths is from femtoseconds to attoseconds, both dispersive and nonlinear effects influence their shape and spectrum.

The following full-wave equation is usually a starting point for mathematical models:

$$\nabla^2 \mathbf{E} - \frac{1}{c^2} \mathbf{E}_{tt} = \mu_0 \mathbf{P}_{tt}, \quad (1.1)$$

which originates directly from Maxwell's equation. If we assume a local medium response and only a third-order nonlinear effect, the so-called Kerr effect, which is the induced polarization, consists of linear and nonlinear parts,  $\mathbf{P}(\mathbf{r}, t) = \mathbf{P}_L(\mathbf{r}, t) + \mathbf{P}_{NL}(\mathbf{r}, t)$ .

Under the assumption of quasi-monochromatic light and a one-dimensional harmonic oscillator, one can derive the nonlinear Schrödinger (NLS) equation,

$$iq_z + \alpha_1 q_{\tau\tau} + \alpha_2 |q|^2 q = 0, \quad (1.2)$$

to govern the slowly varying envelop of optical waves in weakly nonlinear dispersive media [6,7] by assuming  $\mathbf{E} = (1/2)\mathbf{e}_1(q(z, t)e^{-i(\omega_0 t - k_0 z)} + c.c.)$ , where  $\omega_0$  and  $k_0$  represent the central frequency and central wavenumber, respectively, and  $\mathbf{e}_1$  stands for the direction of polarization. Here  $\alpha_1$  represents the effect of group velocity dispersion ( $\alpha_1 > 0$  corresponds to the anomalous dispersion, or the focusing case, and  $\alpha_1 < 0$  corresponds to the normal dispersion, or the defocusing case) and  $\alpha_2 > 0$  represents the self-phase modulation due to the Kerr effect.

Upon switching the spatial and temporal variables and normalization, the NLS equation can be put into a standard form

$$iq_t + \frac{1}{2}q_{xx} + \sigma|q|^2q = 0, \quad (1.3)$$

where  $\sigma = \pm 1$ , which has become a generic model equation, describes the evolution of small amplitude and slowly varying wave packets in weakly nonlinear media [3–5,8,9]. This arises in a variety of physical contexts, such as the nonlinear optics mentioned above, Bose–Einstein condensates [10], water waves [11] and plasma physics [12]. The integrability, as well as the bright soliton solution in the focusing case ( $\sigma = 1$ ), was found by Zakharov & Shabat [13]. The dark soliton solution was found in the defocusing NLS equation ( $\sigma = -1$ ) [7] and was observed experimentally in 1988 [14,15]. Recently, rogue (freak) waves were discovered and the Peregrine soliton was found in the focusing NLS equation [16].

When the width of optical pulses is less than 1 ps, higher-order nonlinear effects have to be taken into account and the NLS equation should be modified. As a result, a generalized NLS (gNLS) equation [4]

$$iq_z + \frac{1}{2}q_{\tau\tau} + \sigma|q|^2q + i(\beta_1 q_{\tau\tau\tau} + \beta_2 \sigma|q|^2 q_\tau + \beta_3 \sigma q(|q|^2)_\tau) = 0 \quad (1.4)$$

can be derived where  $\beta_1$ ,  $\beta_2$  and  $\beta_3$  are the parameters related to the third-order dispersion, self-steepening and stimulated Raman scattering, respectively. Because of its complexity, the study of the gNLS equation is mainly restricted to numeric solutions. However, in some special cases, the gNLS equation becomes integrable and is available for rigorous analysis. To be specific, when  $\beta_1 = \beta_3 = 0$ , the gNLS equation is called the derivative NLS equation, which is integrable. In addition, there are two other integrable cases, i.e.  $\beta_1 : \beta_2 : \beta_3 = 1 : 6 : 0$  (the Hirota equation [17]) and  $\beta_1 : \beta_2 : \beta_3 = 1 : 6 : 3$  (the Sasa–Satsuma equation [18]).

However, when the width of the optical pulse is of the order of sub-femtoseconds (less than  $10^{-15}$  s), then the width of its spectrum is of the order of greater than  $10^{15} \text{ s}^{-1}$ , being comparable

to the spectral width of the optical pulses, and the quasi-monochromatic assumption is not valid anymore. Therefore, compared with the NLS-related models, we need different approaches to derive the mathematical models of ultra-short pulses. To this end, by using the Kramers–Kronig relation of the response function, two groups of Russian researchers obtained a normalized model equation

$$E_{zz} - E_{tt} = E + (|E|^2 E)_{tt}, \quad (1.5)$$

as well as a non-integrable model equation

$$2E_{z\tau} = E + (|E|^2 E)_{\tau\tau}, \quad (1.6)$$

where  $\tau = t - z$ . The solitary-wave solutions and their interactions for the above models were studied in detail in [19–22]. Similarly, Schäfer & Wayne [23] proposed a so-called short-pulse equation to describe the propagation of ultra-short optical pulses in a silicon fibre,

$$u_{xt} = u + \frac{1}{6}(u^3)_{xx}. \quad (1.7)$$

Here,  $u = u(x, t)$  is a real-valued function, representing the magnitude of the optical field. It is completely integrable [24], possessing periodic and soliton solutions [25]. The wave-breaking phenomenon was studied in [26]. The integrable discretization of the short-pulse equation and its geometric formulation was studied in [27,28].

Similar to the NLS equation, the complex representation has advantages for the description of optical waves since a single complex-valued function can contain information about the amplitude and phase of a wave packet simultaneously. Consequently, a complex short-pulse (CSP) equation,

$$q_{xt} + q + \frac{1}{2}\sigma(|q|^2 q_x)_x = 0, \quad (1.8)$$

was proposed by [29,30]. Here  $q = q(x, t)$  is a complex-valued function, representing the optical wave packets in the ultra-short-pulse regime  $\sigma = \pm 1$ , where  $+1$  represents the focusing case and  $-1$  represents the defocusing case. The CSP equation (1.8) can be viewed as an analogue of the NLS equation in the ultra-short-pulse regime.

For the focusing CSP equation, its multi-bright soliton solution was found firstly in Pfaffian form in [29] by Hirota's bilinear method, and soon after in determinant form in [31] by the Kadomtsev–Petviashvili (KP) hierarchy reduction method. In addition to the above multi-bright soliton solution, the multi-breather and the higher-order rogue wave solutions were constructed via the Darboux transformation (DT) method [32]. The gauge transformation of the CSP equation was recently studied in [33]. By formulating the Riemann–Hilbert problem, the inverse scattering transform (IST) for the CSP equation was investigated in [34] and the long-time asymptotic behaviour was analysed in [35].

For the defocusing CSP equation, its multi-dark soliton solution was constructed by the generalized DT method [30] and the KP hierarchy reduction method [36], respectively. Periodic and soliton solutions for both the focusing and defocusing CSP equation were studied in [37]. In [31,36], a geometric formulation of the complex coupled dispersionless (CCD) equation and a geometric interpretation for the hodograph transformation were given for the focusing and defocusing CSP equation, respectively. It is noted that, if we interchange the spatial variable  $x$  and the temporal variable  $t$ , the CCD equation becomes the complex sine-Gordon equation [38] or the  $AB$  system [39], which is the first negative flow of the Ablowitz–Kaup–Newell–Segur system.

Much attention has been paid to the study of discrete integrable systems [40]. This can be traced back to the mid-1970s, when Hirota discretized various famous soliton equations such as the Korteweg–de Vries, modified Korteweg–de Vries and sine-Gordon equations through Hirota's bilinear method [41]. In the past two decades, the field of discrete systems has grown to prominence as an area in which numerous breakthroughs have taken place, inspiring new developments in other areas of mathematics and physics. Among integrable discrete systems, a

complex-valued equation, the so-called Ablowitz–Ladik (AL) lattice equation,

$$iq_{n,t} = (1 + \sigma|q_n|^2)(q_{n+1} + q_{n-1}), \quad (1.9)$$

originally derived by Ablowitz & Ladik [42,43], plays an important role in driving the study of discrete systems. This is the integrable discretization of the NLS equation. Similar to its continuous counterpart, it is known that the AL lattice equation admits the bright soliton solution for the focusing case ( $\sigma = 1$ ) [44,45] and the dark soliton solution for the defocusing case ( $\sigma = -1$ ) [46]. The IST has been developed by several authors [47–50]. The rogue wave solutions to the AL lattice and coupled AL lattice equations were constructed by the DT method [51,52] and by Hirota’s bilinear method [53]. The geometric construction of the AL lattice equation was given by Doliwa & Santini [54]. Besides being used as the basis for numerical schemes for its continuous counterpart, the AL lattice equation also has numerous physical applications, related to the dynamics of anharmonic lattices [55], self-trapping on a dimer [56], Heisenberg spin chains [57], etc.

A question naturally arises: what is the integrable discretization of the CSP equation as an analogue of the AL lattice equation? As a matter of fact, an answer to this question has been given and a semi-discrete CSP (sdCSP) equation, which can be written in a coupled two-component system

$$\text{and } \left. \begin{aligned} \frac{d}{dt}(q_{n+1} - q_n) &= \frac{1}{2}(x_{n+1} - x_n)(q_{n+1} + q_n) \\ \frac{d}{dt}(x_{n+1} - x_n) + \frac{1}{2}\sigma(|q_{n+1}|^2 - |q_n|^2) &= 0, \end{aligned} \right\} \quad (1.10)$$

has been proposed by one of the authors [58,59]. This lattice equation is a semi-discrete analogue of the CSP equation, where the spatial variable is discretized and the time variable remains continuous. It is noted that the above sdCSP equation can also be written as a single equation

$$\frac{d}{dt} \frac{q_{n+1} - q_n}{\Delta x_n} + \frac{1}{2}(q_{n+1} + q_n) + \frac{\sigma}{2} \frac{1}{\Delta x_n} \left( |q_{n+1}|^2 \frac{q_{n+2} - q_{n+1}}{\Delta x_{n+1}} - |q_n|^2 \frac{q_{n+1} - q_n}{\Delta x_n} \right) = 0, \quad (1.11)$$

where  $q_n = q(x_n, t)$ ,  $\Delta x_n = x_{n+1} - x_n$ .

As an analogue to the AL lattice equation in the ultra-short-pulse regime, it is imperative to study this new integrable sdCSP equation because of its potential applications in physics. However, compared with the results for the continuous CSP equation and the AL lattice equation, the sdCSP equation has been studied much less. As far as we are concerned, only the bright soliton solution was derived through Hirota’s bilinear method [59]. Are there dark, breather and rogue wave solutions to this newly integrable semi-discrete equation? On the other hand, this sdCSP equation is the first example of the integrable discrete systems with both the complex dependent variable and hodograph transformation involved. What are the differences and similarities between this sdCSP equation and other integrable discrete systems including the AL lattice equation?

The motivation for the present work is to answer the above questions. To this end, we intend to construct various soliton solutions with vanishing and non-vanishing boundary conditions via the generalized DT method. The remainder of the paper is organized as follows. In §2, a generalized DT of the sdCSP equation was derived through the loop group method [60]. Based on the generalized DT, we obtain the general solitonic formula for the sdCSP equation. Moreover, together with the reciprocal transformation, we will construct the general solitonic formula for the sdCSP equation in terms of the determinant representation. More specifically, starting from the zero seed solution, the  $N$ -bright soliton solution for the focusing case with a zero boundary condition is constructed in §3, while, from the non-zero seed solution, the general  $N$ -dark soliton solution for the defocusing case is derived with a non-zero boundary condition in §4. In §5, the multi-breather solution with a non-zero boundary condition is constructed for the focusing sdCSP equation. Further, it is shown that multi-breather solutions for the focusing sdCSP equation converge to the ones for the continuous counterpart by taking the spatial mesh to zero. Based on

the multi-breather solution, we further derive general high-order rogue wave solutions in §6. Section 7 is devoted to the conclusion and discussions.

## 2. Generalized Darboux transformation for the semi-discrete complex short-pulse equation

The DT, originating from the work of Darboux in 1882 on the Sturm–Liouville equation, is a powerful method for constructing solutions for integrable systems [61]. However, the classical DT cannot be iterated with the same spectral parameters to obtain the multi-dark, breather and higher-order rogue wave solutions. To overcome this difficulty, one of the authors generalized the classical DT by using a limit technique [62], which can be used to yield these solutions. It is noted that, in 2019, various soliton solutions were found for the non-local NLS equation [63]. In this paper, we aim to find soliton solutions for the sdCSP equation (1.11) by the generalized DT. It should be pointed out that the DT and soliton solutions for the semi-discrete coupled dispersionless equation were constructed by [64].

As mentioned in [58], the sdCSP equation can be constructed in a very direct way. It is shown in [30,36] that the CSP equation is related to the CCD equation,

$$q_{ys} = \rho q, \quad \rho_s + \frac{1}{2}\sigma(|q|^2)_y = 0, \quad (2.1)$$

by a reciprocal (hodograph) transformation in the form  $dx = \rho dy - (1/2)\sigma|q|^2 ds$ ,  $dt = -ds$ . The CCD equation [30,32] admits a Lax pair of the form

$$\Psi_y = U(\rho, q; \lambda)\Psi, \quad \Psi_s = V(q; \lambda)\Psi, \quad (2.2)$$

where

$$U(q, \rho; \lambda) = \frac{1}{\lambda} \begin{bmatrix} -i\rho & -\sigma q_y^* \\ q_y & i\rho \end{bmatrix}, \quad V(q; \lambda) = \frac{i}{4}\lambda\sigma_3 + \frac{i}{2}Q, \quad Q = \begin{bmatrix} 0 & -\sigma q^* \\ q & 0 \end{bmatrix}, \quad (2.3)$$

with  $*$  representing the complex conjugate,  $\sigma_3 = \text{diag}(1, -1)$  being the third Pauli matrix. Replacing the forward-difference with the first-order derivative in the spatial part of the Lax pair, i.e.

$$\frac{\Psi_{n+1} - \Psi_n}{a} = \lambda^{-1} \begin{bmatrix} -i\rho_n & -\sigma \frac{q_{n+1}^* - q_n^*}{a} \\ \frac{q_{n+1} - q_n}{a} & i\rho_n \end{bmatrix} \Psi_n,$$

one yields the Lax pair for the semi-discrete CCD equation

$$\Psi_{n+1} = U_n \Psi_n, \quad \Psi_{n,s} = V_n \Psi_n, \quad (2.4)$$

where

$$U_n = \begin{bmatrix} 1 - \frac{ia\rho_n}{\lambda} & -\sigma \frac{q_{n+1}^* - q_n^*}{\lambda} \\ \frac{q_{n+1} - q_n}{\lambda} & 1 + \frac{ia\rho_n}{\lambda} \end{bmatrix}, \quad V_n = \frac{i}{4}\lambda\sigma_3 + \frac{i}{2}Q_n, \quad Q_n = \begin{bmatrix} 0 & \sigma q_n^* \\ q_n & 0 \end{bmatrix}. \quad (2.5)$$

The compatibility condition gives exactly the semi-discrete CCD equation. Replacing  $a\rho_n$  by  $x_{n+1} - x_n$ , one obtains the sdCSP equation (1.10).

Based on the Lax pair of the sdCSP equation (2.4), we derive the DT by the following proposition.

**Proposition 2.1.** *The Darboux matrix*

$$T_n = I + \frac{\lambda_1^* - \lambda_1}{\lambda - \lambda_1^*} P_n, \quad P_n = \frac{|y_{1,n}\rangle \langle y_{1,n}|}{\langle y_{1,n}| |y_{1,n}\rangle}, \quad J = \text{diag}(1, \sigma), \quad (2.6)$$

can convert system (2.4) into a new one,

$$\Psi_{n+1}^{[1]} = U_n(\rho_n^{[1]}, q_n^{[1]}; \lambda) \Psi_n^{[1]}, \quad \Psi_{n,s}^{[1]} = V_n(\rho_n^{[1]}, q_n^{[1]}; \lambda) \Psi_n^{[1]},$$

where  $|y_{1,n}\rangle = (\psi_{1,n}, \phi_{1,n})^T$  is a special solution for system (2.4) with  $\lambda = \lambda_1$ ,  $|y_{1,n}\rangle^\dagger = \langle y_{1,n}|$ . The Bäcklund transformations between  $(\rho_n^{[1]}, q_n^{[1]})$  and  $(\rho_n, q_n)$  are given through

$$\left. \begin{aligned} \rho_n^{[1]} &= \rho_n - \frac{2}{a} \ln_s \left( \frac{E(\langle y_{1,n}| |y_{1,n}\rangle)}{\langle y_{1,n}| |y_{1,n}\rangle} \right) \\ \text{and } q_n^{[1]} &= q_n + \frac{(\lambda_1^* - \lambda_1) \psi_{1,n}^* \phi_{1,n}}{\langle y_{1,n}| |y_{1,n}\rangle} \quad \text{and} \quad |q_n^{[1]}|^2 = |q_n|^2 + 4\sigma \ln_{ss} \left( \frac{\langle y_{1,n}| |y_{1,n}\rangle}{\lambda_1^* - \lambda_1} \right), \end{aligned} \right\} \quad (2.7)$$

and the symbol  $E$  denotes the shift operator  $n \rightarrow n + 1$ .

Assume that we have  $N$  different solutions  $|y_{i,n}\rangle = (\psi_{i,n}, \phi_{i,n})^T$  at  $\lambda = \lambda_i$  ( $i = 1, 2, \dots, N$ ), then we can construct the  $N$ -fold DT and drive the following generalized Darboux matrix. For simplicity, we have omitted the subscript in  $|y_{i,n}\rangle$  and  $\langle y_{i,n}|$ .

**Proposition 2.2.** *The general Darboux matrix can be represented as*

$$T_{n,N} = I + Y M_n^{-1} D^{-1} Y^\dagger, \quad (2.8)$$

where the first subscript,  $n$ , in  $T_{n,N}$  represents the number of eigenvalues in the matrix, the second one,  $N$ , stands for the  $N$ -fold DT,

$$Y = \left[ |y_1^{[0]}\rangle, |y_1^{[1]}\rangle, \dots, |y_1^{[n_1-1]}\rangle, \dots, |y_r^{[0]}\rangle, |y_r^{[1]}\rangle, \dots, |y_r^{[n_r-1]}\rangle \right], \quad N = \sum_{j=1}^r n_j,$$

$$M_n = \begin{bmatrix} M_{11} & M_{12} & \cdots & M_{1r} \\ M_{21} & M_{22} & \cdots & M_{2r} \\ \vdots & \vdots & \ddots & \vdots \\ M_{21} & M_{22} & \cdots & M_{2r} \end{bmatrix}, \quad M_{ij} = \begin{bmatrix} M_{ij}^{[1,1]} & M_{ij}^{[1,2]} & \cdots & M_{ij}^{[1,n_j]} \\ M_{ij}^{[2,1]} & M_{ij}^{[2,2]} & \cdots & M_{ij}^{[2,n_j]} \\ \vdots & \vdots & \ddots & \vdots \\ M_{ij}^{[n_i,1]} & M_{ij}^{[n_i,2]} & \cdots & M_{ij}^{[n_i,n_j]} \end{bmatrix},$$

$$D = \text{diag}(D_1, D_2, \dots, D_r), \quad D_i = \begin{bmatrix} D_i^{[0]} & \cdots & D_i^{[n_i-1]} \\ 0 & \ddots & \vdots \\ 0 & 0 & D_i^{[0]} \end{bmatrix},$$

and

$$|y_i(\lambda_i + \alpha_i \epsilon_i)\rangle = \sum_{k=0}^{n_i-1} |y_i^{[k]}\rangle \epsilon_i^k + O(\epsilon_i^{n_i}), \quad \frac{1}{\lambda - \lambda_i^* - \alpha_i \epsilon_i^*} = \sum_{k=0}^{n_i-1} D_i^{[k]} \epsilon_i^{*k} + O(\epsilon_i^{*n_i}),$$

$$\frac{\langle y_i(\lambda_i + \alpha_i \epsilon_i) | |y_j(\lambda_j + \alpha_j \epsilon_j)\rangle}{\lambda_i^* - \lambda_j + \alpha_i^* \epsilon_i^* - \alpha_j \epsilon_j} = \sum_{k=1}^{n_i} \sum_{l=1}^{n_j} M_{ij}^{[k,l]} \epsilon_i^{*k-1} \epsilon_j^{l-1} + O(\epsilon_i^{*n_i}, \epsilon_j^{n_j}),$$

where the parameters  $\alpha_i$  are the non-zero complex numbers. The general Bäcklund transformations are

$$\left. \begin{aligned} \rho_n^{[N]} &= \rho_n - \frac{2}{a} \ln_s \left( \frac{\det(M_{n+1})}{\det(M_n)} \right) \\ \text{and } q_n^{[N]} &= q_n + \frac{\det(G_n)}{\det(M_n)} \quad \text{and} \quad |q_n^{[N]}|^2 = |q_n|^2 + 4\sigma \ln_{ss}(\det(M_n)), \end{aligned} \right\} \quad (2.9)$$

where  $G_n = \begin{bmatrix} M & Y_k^\dagger \\ -Y_2 & 0 \end{bmatrix}$ ,  $Y_k$  represents the  $k$ th row of matrix  $Y$ .

The proof of propositions 2.1 and 2.2 can be carried out by following the same steps as in [32]. With the aid of the generalized DT, one can construct more general analytical solutions from the trivial solution of the original equation. Departing from the zero seed solution, single and multi-bright soliton solutions can be constructed for the focusing sdCSP equation. Starting from the plane-wave seed solution, the multi-breather and high-order rogue wave solutions can be derived for the focusing sdCSP equation, while one-, two- and multi-dark soliton solutions can be obtained for the defocusing sdCSP equation. The detailed results and the explicit expressions, as well as dynamics for these solutions, are presented in the following two sections.

On account of (2.7), the coordinate transformation between  $x_n^{[N]}$  and  $x_n$  can be represented as

$$x_n^{[N]} = x_n - 2 \ln_s(\det(M_n)), \quad (2.10)$$

where  $x_n$  represents the original coordinates. The second equation in (2.7) and the discrete hodograph transformation (2.10) constitute the solutions for the sdCSP equation (1.11).

### 3. Single and multi-bright solutions

In this section, we construct the exact solution through formula (2.9) as the application of DT. The general bright soliton will be constructed for the focusing CSP equation ( $\sigma = 1$ ). To this end, we start with a seed solution  $\rho_n^{[0]} = \gamma/2$ ,  $q_n^{[0]} = 0$ ,  $\gamma > 0$ . The coordinates for the sdCSP (1.11) can be obtained as  $x_n(s) = \frac{\gamma}{2}na$ ,  $t = -s$ . Solving the Lax pair equation (2.4) with  $(\rho_n, q_n; \lambda) = (\rho_n^{[0]}, q_n^{[0]}; \lambda_i = \alpha_i + i\beta_i)$ ,  $\beta_i > 0$ , one obtains a special solution

$$|y_{i,n}\rangle = \begin{bmatrix} e^{\theta_{i,n}} \\ 1 \end{bmatrix}, \quad \theta_{i,n} = \frac{i}{2}\lambda_i s + n \ln \left( \frac{\lambda_i - (ia\gamma/2)}{\lambda_i + (ia\gamma/2)} \right) + a_i, \quad (3.1)$$

where  $a_i$  are complex parameters. Then one can obtain the single-soliton solution through the formula (2.9)

$$\begin{aligned} \rho_n^{[1]} &= \frac{\gamma}{2} + \frac{\beta_1}{a} [\tanh(\theta_{1,n+1}^R) - \tanh(\theta_{1,n}^R)], & q_n^{[1]} &= \beta_1 \operatorname{sech}(\theta_{1,n}^R) \exp\left(-i\theta_{1,n}^I - \frac{\pi}{2}i\right), \\ x_n^{[1]} &= \frac{\gamma}{2}na + \beta_1 \tanh(\theta_{1,n}^R), & t &= -s, \end{aligned}$$

where the superscripts  $R, I$  represent the real part and imaginary part, respectively,

$$\begin{aligned} \theta_{1,n}^R &= \frac{n}{2}g_1 - \frac{\beta_1}{2}s + a_1^R, \\ \theta_{1,n}^I &= \frac{\alpha_1 s}{2} + n \arg \left( \frac{\lambda_1 - \frac{ia\gamma}{2}}{\lambda_1 + \frac{ia\gamma}{2}} \right) + a_1^I, \\ g_1 &= \ln \left( \frac{4\alpha_1^2 + (2\beta_1 - a\gamma)^2}{4\alpha_1^2 + (2\beta_1 + a\gamma)^2} \right), \end{aligned}$$

where  $4\alpha_1^2 + (2\beta_1 - a\gamma)^2 \neq 0$ . The soliton  $|q_n^{[1]}|^2$  propagates along the line  $\theta_{1,n}^R = 0$ . The peak  $|q_n^{[1]}|_{\max}^2 = \beta_1^2$  is located at  $(x, t) = (n, (1/\beta_1)(ng_1 + 2a_1^R))$ . To obtain the smooth bright soliton for the sdCSP equation, we require that  $\rho_n^{[1]} > 0$  for all  $n \in \mathbf{Z}$  and  $t \in \mathbf{R}$ . Otherwise, the bright soliton will be either a cusp-type or loop-type soliton solution.

If  $\rho_n^{[1]} > 0$  we have the smooth soliton; if  $\rho_n^{[1]} < 0$  we have the loop soliton while  $\rho_n^{[1]} = 0$  corresponds to the cuspon solution. For small enough  $a$ ,  $n$  can be viewed as an approximately continuous variable. Then in the single-soliton case

$$\rho_n^{[1]} \approx \frac{\partial}{\partial n}(x_n^{[1]}) = \frac{\gamma}{2}a + \frac{\beta_1 \operatorname{sech}^2(\theta_{1,n}^R)g_1}{2} \geq \frac{\gamma}{2}a + \frac{\beta_1 g_1}{2} \quad (3.2)$$

under the condition  $g_1 < 0$ . Thus solving the equation  $(\gamma/2)a + \beta_1 g_1/2 = 0$  will yield the parameter condition for the cuspon or loop bright soliton.

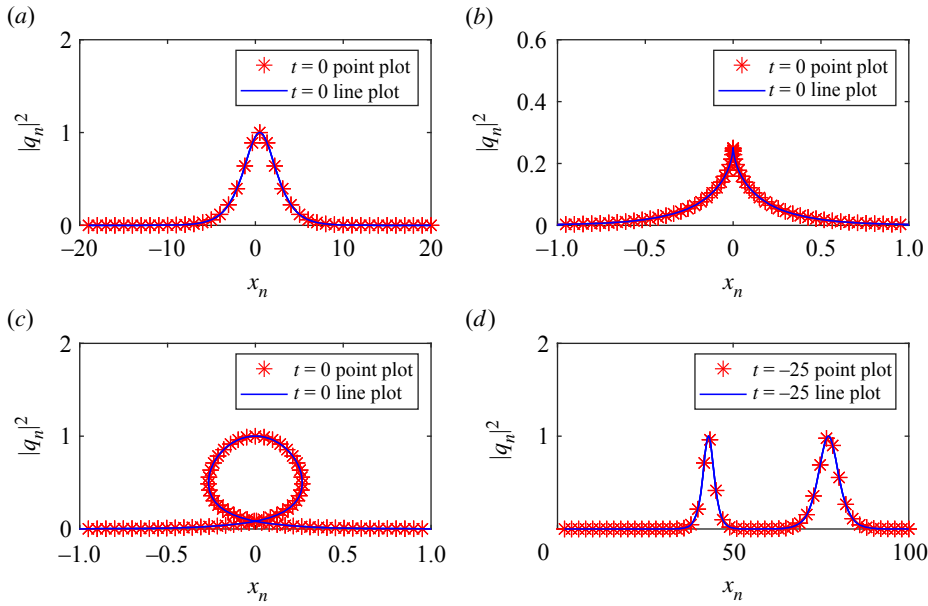


**Figure 1.** (a) Regular bright soliton, (b) cuspon and (c) loop soliton, and (d) two bright soliton. (Online version in colour.)

A regular bright soliton is plotted in figure 1a with parameters  $\gamma = 1$ ,  $a = 2$ ,  $\alpha_1 = 2$ ,  $\beta_1 = 1$ ,  $a_1 = 0$ , a cuspon-type solution is illustrated in figure 1b with parameters  $\gamma = 1$ ,  $a = 1/10$ ,  $\alpha_1 = 0.499$ ,  $\beta_1 = 1/2$ ,  $a_1 = 0$  and a loop soliton is shown in figure 1c with parameters  $\gamma = 1$ ,  $a = 1/10$ ,  $\alpha_1 = 0$ ,  $\beta_1 = 1$ ,  $a_1 = 0$ .

Inserting equation (3.1) into formula (2.9), we can deduce the multi-bright soliton solution as follows:

$$\left. \begin{aligned} \rho_n^{[N]} &= \frac{\gamma}{2} - \frac{2}{a} \ln_s \left( \frac{\det(M_{n+1})}{\det(M_n)} \right), & q_n^{[N]} &= \frac{\det(G_n)}{\det(M_n)} \\ x_n^{[N]} &= \frac{\gamma}{2} na - 2 \ln_s \det(M_n), & t &= -s, \end{aligned} \right\} \quad (3.3)$$

and

where

$$M_n = \left( \frac{e^{\theta_{i,n}^* + \theta_{j,n}} + 1}{\lambda_i^* - \lambda_j} \right)_{1 \leq i, j \leq N}, \quad G_n = \begin{bmatrix} M_n & Y_{1,n}^\dagger \\ -Y_{2,n} & 0 \end{bmatrix},$$

$$Y_{1,n} = [e^{\theta_{1,n}}, e^{\theta_{2,n}}, \dots, e^{\theta_{N,n}}], \quad Y_{2,n} = [1, 1, \dots, 1],$$

and the expression for  $\theta_{i,n}$  is given in (3.1).

In what follows, we will prove that the multi-bright soliton solution of the sdCSP equation converges to the multi-bright soliton solution of the continuous CSP equation obtained in [31,32]. Referring to the Taylor expansion

$$\ln(1 \pm x) = \pm x + o(x^2), \quad (3.4)$$

we have

$$n \ln \left( \frac{\lambda_i - (ia\gamma/2)}{\lambda_i + (ia\gamma/2)} \right) \approx -n \frac{ia\gamma}{\lambda_i} = -\frac{i\gamma}{\lambda_i} y \quad (3.5)$$

by letting  $na = y$  in the continuous limit  $a \rightarrow 0$ . Therefore,  $\theta_{i,n}$  agrees with eqn (32) in [32] by noticing the correspondence  $\theta_{i,n} \rightarrow 2\theta_{i,n}$  and  $\gamma \rightarrow -\gamma$ .

In particular, we give the two-soliton solution explicitly through the above general formula (3.3),

$$\left. \begin{aligned} \rho_n^{[2]} &= \frac{\gamma}{2} - \frac{2}{a} \ln_s \left( \frac{\det(M_{n+1}^{[2]})}{\det(M_n^{[2]})} \right), \quad q_n^{[2]} = \frac{\det(G_n^{[2]})}{\det(M_n^{[2]})} \\ \text{and} \quad x_n^{[2]} &= \frac{\gamma}{2} na - 2 \ln_s \det(M_n^{[2]}), \quad t = -s, \end{aligned} \right\} \quad (3.6)$$

where

$$\begin{aligned} M_n^{[2]} &= \frac{(e^{\theta_{1,n} + \theta_{1,n}^*} + 1)(e^{\theta_{2,n} + \theta_{2,n}^*} + 1)}{4\beta_1\beta_2} - \frac{(e^{\theta_{2,n} + \theta_{1,n}^*} + 1)(e^{\theta_{1,n} + \theta_{2,n}^*} + 1)}{(\alpha_2 - \alpha_1)^2 + (\beta_1 + \beta_2)^2}, \\ G_n^{[2]} &= \left( \frac{e^{\theta_{2,n} + \theta_{1,n}^*} + 1}{(\beta_1 + \beta_2) + i(\alpha_1 - \alpha_2)} - \frac{e^{\theta_{1,n} + \theta_{1,n}^*} + 1}{2\beta_1} \right) e^{\theta_{2,n}^*} \\ &\quad + \left( \frac{e^{\theta_{1,n} + \theta_{2,n}^*} + 1}{(\beta_1 + \beta_2) + i(\alpha_2 - \alpha_1)} - \frac{e^{\theta_{2,n} + \theta_{2,n}^*} + 1}{2\beta_2} \right) e^{\theta_{1,n}^*}. \end{aligned}$$

The profile of the two regular soliton solution is shown in figure 1d with parameters  $\gamma = 2$ ,  $a = 2$ ,  $\alpha_1 = 2$ ,  $\beta_1 = 1$ ,  $a_1 = 0$ ,  $\alpha_2 = 1$ ,  $\beta_2 = 1$ ,  $a_2 = 0$ . It can be seen that the two regular solitons coexist in a fixed time. Actually, they will interact with each other elastically as time goes on.

## 4. Single and multi-dark soliton solutions

In this section, we construct the single and multi-dark soliton solutions for the defocusing sdCSP equation ( $\sigma = -1$ ). Generally, the DT cannot apply to derive the dark solitons directly since the spectral points of dark solitons are located in the real axis and the Darboux matrix is trivial if  $\lambda_1 = \lambda_1^*$ . One of the authors [65] developed a method to yield the dark soliton and multi-dark solitons through a limit technique based on [66]. In what follows, we derive the single dark and multi-dark solitons for the sdCSP equation by following the steps in [65].

Starting from the seed solution in the form of a plane wave

$$\rho_n^{[0]} = \frac{\gamma}{2}, \quad q_n^{[0]} = \frac{\beta}{2} e^{i\theta_n}, \quad \theta_n = bn + \frac{c}{2}s, \quad c = \frac{a\gamma}{2} \frac{\sin(b)}{\cos(b) - 1}, \quad \gamma > 0, \quad \beta \geq 0, \quad b \neq k\pi, \quad k \in \mathbb{Z}, \quad (4.1)$$

we can derive the solution vector for the Lax pair equation (2.4) with  $(q_n, \rho_n; \lambda) = (q_n^{[0]}, \rho_n^{[0]}; \lambda_i)$

$$|y_{i,n}\rangle = KL_i E_i = K \begin{bmatrix} \widehat{\phi}_{i,n} \\ \beta \widehat{\psi}_{i,n} \end{bmatrix}, \quad K = \text{diag} \left( e^{-(i/2)\theta_n}, e^{(i/2)\theta_n} \right), \quad \lambda_i \neq -c + i\beta, \quad (4.2)$$

where  $|y_{i,n}\rangle$  is a special solution of the Lax pair with a non-zero seed solution by discarding a function,

$$L_i = \begin{bmatrix} 1 & 1 \\ \beta & \beta \\ c + \chi_i^+ & c + \chi_i^- \end{bmatrix}, \quad E_i = \begin{bmatrix} e^{\omega_{i,n}} \\ \alpha_i(\bar{\lambda}_i - \lambda_i)e^{-\omega_{i,n}} \end{bmatrix}$$

and

$$\left. \begin{aligned} \omega_{i,n} &= \frac{i}{4}\xi_i s + \frac{n}{2} \ln \left( \frac{\sin(b/2)((1/2)a\gamma - \xi_i) + i \cos(b/2)\lambda_i}{\sin(b/2)((1/2)a\gamma + \xi_i) + i \cos(b/2)\lambda_i} \right) + a_i \\ \text{and} \quad \chi_i^\pm &= \lambda_i \pm \xi_i, \quad \xi_i = \sqrt{(\lambda_i + c)^2 - \beta^2}, \end{aligned} \right\} \quad (4.3)$$

where  $\alpha_i$ 's are appropriate complex parameters and  $a_i$ 's are real parameters. In order to derive the single dark soliton solution, we consider only  $\lambda_1$  and reparametrize  $\chi_1^\pm$  and  $\xi_1$  in (4.3) by

$$\chi_1^\pm = \beta[\cos(\varphi_1) \pm i \sin(\varphi_1)], \quad \xi_1 = i\beta \sin(\varphi_1), \quad (4.4)$$

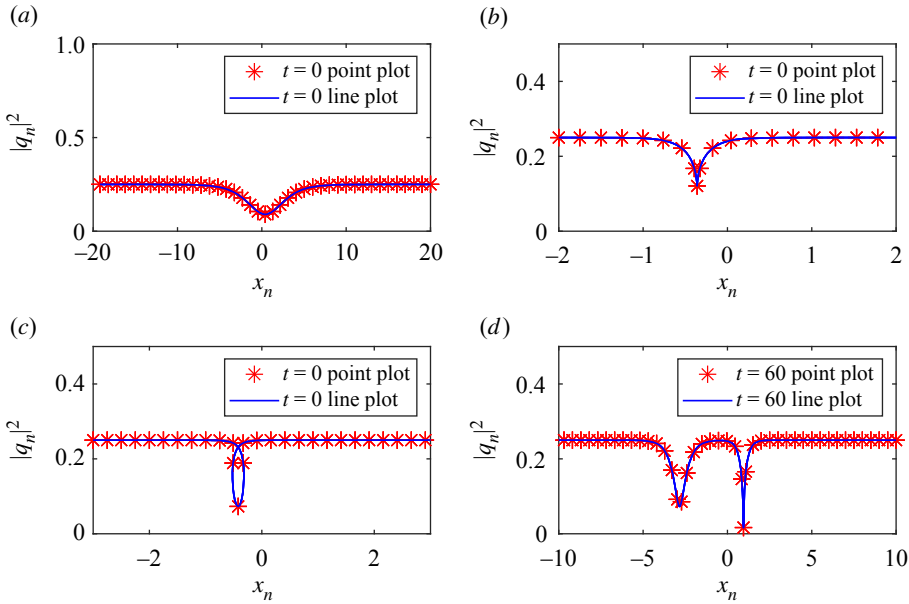


**Figure 2.** (a) Regular dark soliton, (b) cuspon and (c) loop dark soliton, and (d) two dark soliton. (Online version in colour.)

with  $0 < \varphi_i < \pi$ ,  $a_i \in \mathbb{R}$ . By taking a limit process  $\lambda_1 \rightarrow \bar{\lambda}_1$  similar to the one in [65], the single dark soliton solution can be obtained as follows:

$$\left. \begin{aligned} \rho_n^{[1]} &= \frac{\gamma}{2} + \frac{\beta}{2a} \sin(\varphi_1) (\tanh(Z_{1,n+1}) - \tanh(Z_{1,n})), \\ q_n^{[1]} &= \frac{\beta}{2} \left[ 1 - i \sin(\varphi_1) e^{-i\varphi_1} - i \sin(\varphi_1) e^{-i\varphi_1} \tanh(Z_{1,n}) \right] e^{i\theta_n} \\ x_n^{[1]} &= \frac{\gamma}{2} a n + \frac{\beta^2}{8} s + \frac{\beta}{2} \sin(\varphi_1) \tanh(Z_{1,n}), \quad t = -s, \end{aligned} \right\} \quad (4.5)$$

and

where

$$Z_{1,n}(\varphi_1, a_1) = \frac{n}{2} \ln(A) - \frac{\beta}{4} \sin(\varphi_1) s + a_1, \quad A = \frac{a\gamma + 2\beta \sin((1/2)b) \cos((1/2)b + \varphi_1)}{a\gamma + 2\beta \sin((1/2)b) \cos((1/2)b - \varphi_1)} \quad (4.6)$$

and  $a_1$  is a real parameter,  $A > 0$ .

Similar to the bright case, the single dark soliton becomes a cuspon if  $\rho_n^{[1]} = 0$  or a loop type if  $\rho_n^{[1]} < 0$ . The cuspon and loop-type dark solitons can be defined by the sign of  $\rho_n^{[1]} \approx (\partial/\partial n)x_n^{[1]}$  with  $a$  small enough. For the single dark soliton, it follows from

$$\frac{\partial}{\partial n} x_n^{[1]} = \frac{a\gamma}{2} + \frac{\beta}{4} \sin(\varphi_1) \ln(A) \operatorname{sech}^2(Z_{1,n}) \geq \frac{a\gamma}{2} + \frac{\beta}{4} \sin(\varphi_1) \ln(A) \quad (4.7)$$

that the condition  $a\gamma/2 + (\beta/4) \sin(\varphi_1) \ln(A) = 0$  determines the types of dark solitons.

As examples, we plot cuspon- and loop-type dark solitons in figure 2b,c, respectively. The parameters for the cuspon-type solution are  $a = 1/10$ ,  $b = \pi/2$ ,  $\gamma = 5$ ,  $\beta = 1$ ,  $\varphi_1 = 0.802$ ,  $a_1 = 0$ , while for the loop-type solution the parameters are  $a = 1/10$ ,  $b = \pi/2$ ,  $\gamma = 5$ ,  $\beta = 1$ ,  $\varphi_1 = 1$ ,  $a_1 = 0$ . In figure 2a, we illustrate a regular dark soliton with parameters  $a = 1$ ,  $b = \pi/2$ ,  $\gamma = 2$ ,  $\beta = 1$ ,  $\varphi_1 = \arcsin(4/5)$ ,  $a_1 = 0$ .

Next, we proceed to find  $N$ -dark soliton solutions. Based on the  $N$ -soliton solution (2.9) to the defocusing sdCSP equation, it then follows that

$$\left. \begin{aligned} q_n^{[N]} &= \frac{\beta}{2} \left[ 1 + \widehat{Y}_{2,n} M_n^{-1} \widehat{Y}_{1,n}^\dagger \right] e^{i\theta_n} = \frac{\beta}{2} \left[ \frac{\det(H_n)}{\det(M_n)} \right] e^{i\theta_n} \\ \text{and} \quad x_n &= \frac{\gamma}{2} an + \frac{\beta^2}{8} s - 2 \ln_s(\det(M_n)), \quad t = -s, \end{aligned} \right\} \quad (4.8)$$

where

$$\begin{aligned} M_n &= \left( \frac{\langle y_{i,n} | \sigma_3 | y_{j,n} \rangle}{2(\bar{\lambda}_i - \lambda_j)} \right)_{1 \leq i, j \leq N}, \quad H_n = M_n + Y_{1,n}^\dagger Y_{2,n}, \\ \widehat{Y}_{1,n} &= [\widehat{\phi}_{1,n}, \widehat{\phi}_{2,n}, \dots, \widehat{\phi}_{N,n}], \quad \widehat{Y}_{2,n} = [\widehat{\psi}_{1,n}, \widehat{\psi}_{2,n}, \dots, \widehat{\psi}_{N,n}]. \end{aligned}$$

In general, the above  $N$ -soliton solution (4.8) is singular. In order to derive the  $N$ -dark soliton solution through the DT method, we need to take a limit process  $\lambda_i \rightarrow \bar{\lambda}_i$  ( $i = 1, 2, \dots, N$ ). By a tedious procedure which is omitted here, we finally have the  $N$ -dark soliton solution to the defocusing sdCSP equation (1.11) as follows.

**Proposition 4.1.**

$$\left. \begin{aligned} \rho_n^{[N]} &= \frac{\gamma}{2} - \frac{2}{a} \ln_s \frac{\det(G_{n+1})}{\det(G_n)}, \quad q_n^{[N]} = \frac{\beta}{2} \left[ \frac{\det(H_n)}{\det(G_n)} \right] e^{i\theta_n} \\ \text{and} \quad x_n^{[N]} &= \frac{\gamma}{2} an + \frac{\beta^2}{8} s - 2 \ln_s \det(G_n), \quad t = -s, \end{aligned} \right\} \quad (4.9)$$

where  $G_n = (g_{i,j})_{1 \leq i, j \leq N}$ ,  $H_n = (h_{i,j})_{1 \leq i, j \leq N}$ ,

$$\delta_{ij} = \frac{\delta_{ij} + e^{Z_{i,n} + Z_{j,n}}}{\exp(-i\varphi_i) - \exp(i\varphi_j)}, \quad h_{ij} = \frac{\delta_{ij} + e^{(Z_{i,n} - i\varphi_i) + (Z_{j,n} - i\varphi_j)}}{\exp(-i\varphi_i) - \exp(i\varphi_j)}, \quad (4.10)$$

and  $Z_{i,n} = Z_{1,n}(\varphi_i, a_i)$  and  $\delta_{i,j}$  is the standard Kronecker delta.

By taking  $N = 2$  in (4.9) and (4.10), the determinants corresponding to the two-dark soliton solution can be calculated as

$$|G_n| = 1 + e^{2Z_{1,n}} + e^{2Z_{2,n}} + a_{12} e^{2(Z_{1,n} + Z_{2,n})} \quad (4.11)$$

and

$$|H_n| = 1 + e^{2(Z_{1,n} - i\varphi_1)} + e^{2(Z_{2,n} - i\varphi_2)} + a_{12} e^{2(Z_{1,n} + Z_{2,n} - i\varphi_1 - i\varphi_2)}, \quad (4.12)$$

where

$$a_{12} = \frac{\sin^2((\varphi_2 - \varphi_1)/2)}{\sin^2((\varphi_2 + \varphi_1)/2)}. \quad (4.13)$$

Asymptotic analysis can be easily performed for two-soliton interactions, which shows that the collision is always elastic.

On the other hand, if we choose  $a = 1$ ,  $\gamma = \beta = 1$ ,  $\varphi_1 = 1.31859$ ,  $\varphi_2 = 1$ ,  $a_1 = 0$ ,  $a_2 = 0$ , we then have the interaction between a regular dark and a cuspon-type dark soliton (figure 2d). However, in either case, the interaction between two dark solitons is always elastic, which is verified by the asymptotic analysis.

Before concluding this section, let us prove that the multi-dark solution converges to its counterpart of the continuous CSP equation obtained in [30]. In the continuous limit, we assume that  $a = b \rightarrow 0$ ; it then follows that  $c \rightarrow -\gamma$ . Referring to the Taylor expansion (3.4),  $Z_{i,n}$  turns out

to be

$$\begin{aligned} & \frac{n}{2} \ln \left( \frac{a\gamma + 2\beta \sin((1/2)b) \cos((1/2)b + \varphi_i)}{a\gamma + 2\beta \sin((1/2)b) \cos((1/2)b - \varphi_i)} \right) - \frac{\beta}{4} \sin(\varphi_i)s + a_i \\ & \approx \frac{-2n\beta \sin(b/2) \sin(\varphi_i)}{2\beta \cos(b/2) \cos(\varphi_i) + a\gamma} - \frac{\beta}{4} \sin(\varphi_i)s + a_i. \end{aligned} \tag{4.14}$$

Note that, between the present paper and [30],  $\gamma \rightarrow -\gamma$ . As a result  $Z_{i,n} \rightarrow \omega_i$  in [30] by letting  $nb = y$  and the proof is complete.

### 5. Single-breather and multi-breather solutions

The single-breather and multi-breather solutions for the focusing sdCSP equation (1.11) ( $\sigma = 1$ ) can be constructed from the seed solution/plane-wave solution through formula (2.9). We depart from the seed solution

$$\rho_n^{[0]} = \frac{\gamma}{2}, q_n^{[0]} = \frac{\beta}{2} e^{i\theta_n}, \theta_n = bn + \frac{c}{2}s, c = \frac{a\gamma}{2} \frac{\sin(b)}{\cos(b) - 1}, \gamma > 0, \beta \geq 0. \tag{5.1}$$

The coordinates for sdCSP (1.11) can be obtained as  $x_n(s) = (\gamma/2)na - (\beta^2/8)s$ ,  $t = -s$ . Then we have the solution vector for the Lax pair equation (2.4) ( $\sigma = 1$ ) with  $(q_n, \rho_n; \lambda) = (q_n^{[0]}, \rho_n^{[0]}; \lambda_1)$ ,

$$|y_{1,n}\rangle = KL_1E_1, K = \text{diag} \left( e^{-(i/2)\theta_n}, e^{(i/2)\theta_n} \right), \lambda_1 \neq -c + i\beta, \tag{5.2}$$

where

$$L_1 = \begin{bmatrix} 1 & 1 \\ \beta & \beta \end{bmatrix}, E_i = \begin{bmatrix} e^{\theta_{1,n}} \\ 1 \end{bmatrix}$$

and

$$\left. \begin{aligned} \theta_{1,n} &= \frac{i}{2} \xi_1 s + n \ln \left( \frac{\sin(b/2) ((1/2)ia\gamma - \xi_1) + i \cos(b/2)\lambda_1}{\sin(b/2) ((1/2)ia\gamma + \xi_1) + i \cos(b/2)\lambda_1} \right) + a_1 \\ \eta_1 &= \lambda_1 + \xi_1, \chi_1 = \lambda_1 - \xi_1, \xi_1 = \sqrt{\beta^2 + (\lambda_1 + c)^2}. \end{aligned} \right\} \tag{5.3}$$

The single-breather solution can be constructed from formula (2.9) with the elementary identity introduced in [65],

$$\left. \begin{aligned} \rho_n^{[1]} &= \frac{\gamma}{2} - \frac{2}{a} \ln_s \left( \frac{\cosh(\theta_{1,n+1}^R) \cosh(\varphi_1^R/2) - \sin(\theta_{1,n+1}^I) \sin(\varphi_1^I/2)}{\cosh(\theta_{1,n}^R) \cosh(\varphi_1^R/2) - \sin(\theta_{1,n}^I) \sin(\varphi_1^I/2)} \right), \\ q_n^{[1]} &= \frac{\beta}{2} \left[ \frac{\cosh(\theta_{1,n}^R - i\varphi_1^I) \cosh(\varphi_1^R/2) + \sin(\theta_{1,n}^I + i\varphi_1^R) \sin(\varphi_1^I/2)}{\cosh(\theta_{1,n}^R) \cosh(\varphi_1^R/2) - \sin(\theta_{1,n}^I) \sin(\varphi_1^I/2)} \right] e^{i\theta_n} \end{aligned} \right\} \tag{5.4}$$

and 
$$x_n^{[1]} = \frac{\gamma}{2}na - \frac{\beta^2}{8}s - 2 \ln_s \left( \cosh(\theta_{1,n}^R) \cosh \left( \frac{\varphi_1^R}{2} \right) - \sin(\theta_{1,n}^I) \sin \left( \frac{\varphi_1^I}{2} \right) \right), t = -s,$$

where

$$\begin{aligned} \xi_i &= \beta \cosh \left[ \frac{1}{2}(\varphi_i^R + i\varphi_i^I) \right], \eta_i + c = \beta e^{(1/2)(\varphi_i^R + i\varphi_i^I)}, \chi_i + c = -\beta e^{-(1/2)(\varphi_i^R + i\varphi_i^I)}, \\ \theta_{1,n}^R &= \frac{\ln(\xi_1)}{2}n - \frac{\beta}{2} \sinh \left( \frac{\varphi_1^R}{2} \right) \sin \left( \frac{\varphi_1^I}{2} \right) s - \frac{\varphi_1^R}{2} + a_1^R, \\ \theta_{1,n}^I &= h_1n + \frac{\beta}{2} \cosh \left( \frac{\varphi_1^R}{2} \right) \cos \left( \frac{\varphi_1^I}{2} \right) s - \frac{\varphi_1^I}{2} + a_1^I \end{aligned}$$

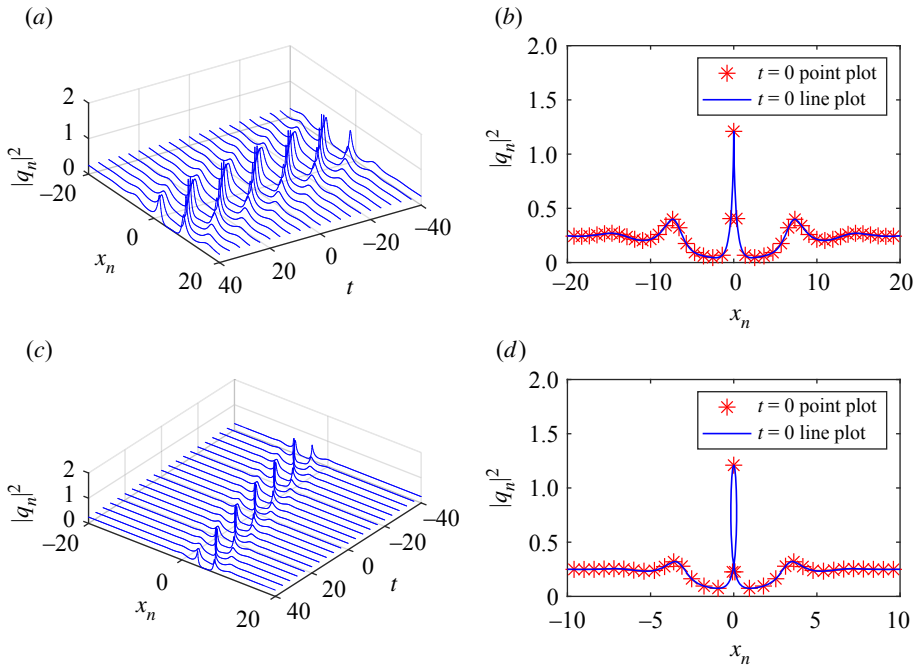


**Figure 3.** (a,b) Cuspon and (c,d) loop Kuznetsov–Ma breather. (Online version colour.)

and

$$g_1 = \frac{\beta^2 \cosh^2(\varphi_1^R/2) \sin^2(b/2 + \varphi_1^I/2) + \left[ \beta \sinh(\varphi_1^R/2) \cos(b/2 + \varphi_1^I/2) + \frac{a\gamma}{2 \sin(b/2)} \right]^2}{\beta^2 \cosh^2(\varphi_1^R/2) \sin^2(b/2 - \varphi_1^I/2) + \left[ \beta \sinh(\varphi_1^R/2) \cos(b/2 - \varphi_1^I/2) + \frac{a\gamma}{2 \sin(b/2)} \right]^2},$$

$$h_1 = \arg \left( \frac{\sin(b/2) \left( (1/2)ia\gamma - \beta \cosh \left[ (1/2)(\varphi_1^R + i\varphi_1^I) \right] \right) + i \cos(b/2) \left( \beta \sinh \left[ (1/2)(\varphi_1^R + i\varphi_1^I) \right] - c \right)}{\sin(b/2) \left( (1/2)ia\gamma + \beta \cosh \left[ (1/2)(\varphi_1^R + i\varphi_1^I) \right] \right) + i \cos(b/2) \left( \beta \sinh \left[ (1/2)(\varphi_1^R + i\varphi_1^I) \right] - c \right)} \right).$$

A technique to fix the maximum peak at the origin is to choose the parameters  $a_1^R = \varphi_1^R/2$  and  $a_1^I = \varphi_1^I/2 + \pi/2$ , which are useful in determining the types of breathers. We should comment here that, depending on  $\rho_n^{[1]}$ , the breather solution may be of regular ( $\rho_n^{[1]} > 0$ ), cuspon ( $\rho_n^{[1]} = 0$ ) or loop type ( $\rho_n^{[1]} < 0$ ). For the single breather, we will find the parameter condition with the value at the origin. Similar to the above sections, we can determine the condition of the cuspon or loop breather by  $\rho_n^{[1]} \approx (\partial/\partial n)x_n^{[1]}$  with  $a$  small enough.

As examples, we show a cuspon breather with parameters  $\beta = 1$ ,  $\gamma = 18.29$ ,  $a = 1/10$ ,  $b = \pi/2$ ,  $\varphi_{1R} = 0$ ,  $\varphi_{1I} = 2 \arcsin(3/5)$ ,  $a_1 = i \arcsin(3/5) + i(\pi/2)$  in figure 3a,b and a loop breather in figure 3c,d with parameters  $\beta = 1$ ,  $\gamma = 12$ ,  $a = 1/10$ ,  $b = \pi/2$ ,  $\varphi_{1R} = 0$ ,  $\varphi_{1I} = 2 \arcsin(3/5)$ ,  $a_1 = i \arcsin(3/5) + i(\pi/2)$ .

Furthermore, by using the  $N$ -fold DT, we derive the  $N$ -breather solution through formula (2.9) and some tedious algebraic calculations, as shown in the following proposition.

**Proposition 5.1.** *The multi-breather solution for the sdCSP equation (1.11) can be represented as*

$$\left. \begin{aligned} \rho_n^{[N]} &= \frac{\gamma}{2} - \frac{2}{a} \ln_s \left( \frac{\det(M_{n+1})}{\det(M_n)} \right), \quad q_n^{[N]} = \frac{\beta}{2} \left[ \frac{\det(G_n)}{\det(M_n)} \right] e^{i\theta_n} \\ x_n^{[N]} &= \frac{\gamma}{2} an - \frac{\beta^2}{8} s - 2 \ln_s \det(M_n), \quad t = -s, \end{aligned} \right\} \quad (5.5)$$

and

where

$$M_n = \left( \frac{e^{\theta_{m,n}^* + \theta_{k,n}}}{\eta_m^* - \eta_k} - \frac{e^{\theta_{m,n}^*}}{\eta_m^* - \chi_k} - \frac{e^{\theta_{k,n}}}{\chi_m^* - \eta_m} + \frac{1}{\chi_m^* - \chi_k} \right)_{1 \leq m, k \leq N},$$

$$G_n = \left( \frac{e^{\theta_{m,n}^* + \theta_{k,n}}}{\eta_m^* - \eta_k} \frac{\eta_m^* + c}{\eta_k + c} - \frac{e^{\theta_{m,n}^*}}{\eta_m^* - \chi_k} \frac{\eta_m^* + c}{\chi_k + c} - \frac{e^{\theta_{k,n}}}{\chi_m^* - \eta_m} \frac{\chi_m^* + c}{\eta_k + c} + \frac{1}{\chi_m^* - \chi_k} \frac{\chi_m^* + c}{\chi_k + c} \right)_{1 \leq m, k \leq N}$$

and the parameters  $\theta_{k,n}$ ,  $\eta_i$ ,  $\chi_i$  are given in equations (4.3).

Finally, we give a proof that the above multi-breather solution converges to the multi-breather solution to the CSP equation obtained in [32]. To this end, we assume  $a = b \rightarrow 0$  in the continuous limit and notice that  $\gamma \rightarrow -\gamma$  compared with the breather solution in [32]. By using the Taylor expansion (3.4),  $\theta_{i,n}$  becomes

$$\frac{i}{2} \xi_i s + n \ln \left( \frac{\sin(b/2) \left( \frac{1}{2} i a \gamma - \xi_i \right) + i \cos(b/2) \lambda_i}{\sin(b/2) \left( (1/2) i a \gamma + \xi_i \right) + i \cos(b/2) \lambda_i} \right) + a_i \quad (5.6)$$

$$\approx \frac{i}{2} \xi_i s - \frac{2n \sin(b/2) \xi_i}{i \cos(b/2) \lambda_i + (1/2) i a \gamma \sin(b/2)} + a_i \quad (5.7)$$

$$= \frac{i}{2} \xi_i s + \frac{i \xi_i}{\lambda_i} y + a_i \quad (5.8)$$

by letting  $nb = y$  in the continuous limit  $b \rightarrow 0$ . This shows how the multi-breather solution to the sdCSP equation converges to the multi-breather solution of the CSP equation in the continuous limit.

## 6. Fundamental and high-order rogue wave solutions

In this section, we proceed to the construction of the general rogue wave solution for the focusing sdCSP equation based on the general breather solution obtained in the previous section. It is inconvenient to start off the calculation in the same way as the previous one since the solution vectors involve the square root of a complex number. To avoid this difficulty, we introduce the following transformation:

$$\lambda_i + c = \beta \sinh \left[ \frac{1}{2} (\varphi_i^R + i \varphi_i^I) \right], \quad (\varphi_i^R, \varphi_i^I) \in \Omega,$$

where  $\Omega = \{(\varphi^R, \varphi^I) | 0 < \varphi^I < \pi, \text{ and } 0 < \varphi^R < \infty, \text{ or } \varphi^R = 0, \text{ and } \pi/2 \leq \varphi^I < \pi\}$ , then

$$\xi_i = \beta \cosh \left[ \frac{1}{2} (\varphi_i^R + i \varphi_i^I) \right], \quad \eta_i + c = \beta e^{(1/2)(\varphi_i^R + i \varphi_i^I)}, \quad \chi_i + c = -\beta e^{-(1/2)(\varphi_i^R + i \varphi_i^I)}.$$

Actually, we can obtain the rogue wave and high-order rogue wave solutions at this special point. The general procedure to yield these solutions was proposed in [62]. The rogue wave solution and the corresponding modulational instability analysis for the vector NLS equations are analysed in [67,68]. If we solve the linear system (2.4) with  $(q_n, \rho_n, \lambda) = (q_n^{[0]}, \rho_n^{[0]}, -c + i\beta)$ , where  $q_n^{[0]}$  and  $\rho_n^{[0]}$  are given in equations (4.1), then the quasi-rational solution vector is obtained. With this solution vector, we could construct the first-order rogue wave solution but fail to obtain the high-order rogue wave solutions. To obtain the general high-order rogue wave solution in a simple way, we must solve the linear system (2.4) with  $(q_n, \rho_n, \lambda) = (q_n^{[0]}, \rho_n^{[0]}, -c + i\beta \cos(\epsilon))$ , where  $\epsilon$  is a small parameter.

Lemma 6.1 is useful in obtaining the general high-order rogue wave solution. Denote

$$\lambda_1 = -c + i\beta \cos(\epsilon), \quad \xi_1 = \beta \sin(\epsilon), \quad \eta_1 = \lambda_1 + \xi_1 = -c + i\beta e^{-i\epsilon}, \quad c = -\frac{1}{2} a \gamma \cot \left( \frac{b}{2} \right). \quad (6.1)$$

**Lemma 6.1.** *The following parameters can be expanded with  $\epsilon$ , where  $\epsilon$  is a small parameter:*

$$\mu_1 = \sum_{n=0}^{\infty} \mu_1^{[n]} \epsilon^{2n+1}, \quad \frac{\beta}{i(\eta_1^* - \eta_1)} = \frac{1}{e^{i\epsilon^*} + e^{-i\epsilon}} = \sum_{i=0, j=0}^{\infty, \infty} F^{[i, j]} \epsilon^{*i} \epsilon^j,$$

where

$$\mu_1^{[n]} = \frac{\beta (-1)^n}{(2n+1)!}, \quad F^{[i, j]} = \frac{1}{i!j!} \frac{\partial^{i+j}}{\partial \epsilon^{*i} \partial \epsilon^j} \left( [e^{i\epsilon^*} + e^{-i\epsilon}]^{-1} \right) \Big|_{\epsilon^* = \epsilon = 0}.$$

With the aid of lemma 6.1, we obtain the following expansion:

$$\begin{aligned} Z_{1,n} &\equiv \frac{i\beta}{4} \sin(\epsilon) s + \frac{n}{2} \ln \left( \frac{\beta \sin((3/2)b - \epsilon) + \beta \sin((1/2)b + \epsilon) - 2i \cos((1/2)b) a\gamma}{\beta \sin((3/2)b + \epsilon) + \beta \sin((1/2)b - \epsilon) - 2i \cos((1/2)b) a\gamma} \right) \\ &\quad - \frac{i\epsilon}{2} + \sum_{i=1}^{\infty} (e_i + i f_i) \epsilon^{2i-1} \\ &= i\epsilon \sum_{k=0}^{\infty} Z_{1,n}^{[2k+1]} \epsilon^{2k}, \quad Z_{1,n}^{[2k+1]} = \frac{d^{2k+1}}{d\epsilon^{2k+1}} Z_{1,n} \Big|_{\epsilon=0}. \end{aligned}$$

Furthermore, we have

$$e^{Z_{1,n}} = \sum_{i=0}^{\infty} S_i(\mathbf{Z}_{1,n}) \epsilon^i, \quad \mathbf{Z}_{1,n} = (Z_{1,n}^{[1]}, Z_{1,n}^{[2]}, \dots), \quad Z_{1,n}^{[2k]} = 0, \quad k \geq 1,$$

where the explicit expression of these polynomials can be given by the elementary Schur polynomials

$$\begin{aligned} S_0(\mathbf{Z}_{1,n}) &= 1, \quad S_1(\mathbf{Z}_{1,n}) = Z_{1,n}^{[1]}, \quad S_2(\mathbf{Z}_{1,n}) = Z_{1,n}^{[2]} + \frac{(Z_{1,n}^{[1]})^2}{2}, \\ S_3(\mathbf{Z}_{1,n}) &= Z_{1,n}^{[3]} + Z_{1,n}^{[1]} Z_{1,n}^{[2]} + \frac{(Z_{1,n}^{[1]})^3}{6}, \dots \\ S_i(\mathbf{Z}_{1,n}) &= \sum_{l_1+2l_2+\dots+kl_k=i} \frac{(Z_{1,n}^{[1]})^{l_1} (Z_{1,n}^{[2]})^{l_2} \dots (Z_{1,n}^{[k]})^{l_k}}{l_1! l_2! \dots l_k!}. \end{aligned}$$

Since  $KE_{1,n}(\epsilon)$  satisfies the Lax equation (2.4), then  $KE_{1,n}(-\epsilon)$  also satisfies the Lax equation (2.4). To obtain the general high-order rogue wave solution, we choose the general special solution

$$|y_{1,n}\rangle = \frac{K}{2\epsilon} [E_{1,n}(\epsilon) - E_{1,n}(-\epsilon)] \equiv K \begin{bmatrix} \varphi_{1,n} \\ \beta \psi_{1,n} \end{bmatrix}, \quad E_{1,n} = \begin{bmatrix} e^{Z_{1,n}} \\ \frac{\beta e^{Z_{1,n}}}{\eta_1 + c} \end{bmatrix}.$$

Finally, we have

$$\begin{aligned} \frac{\beta \langle y_{1,n} | y_{1,n} \rangle}{2i(\lambda_1^* - \lambda_1)} &= \frac{\beta}{4i} \left[ \frac{e^{Z_{1,n}^* + Z_{1,n}}}{\eta_1^* - \eta_1} - \frac{e^{Z_{1,n}^* - Z_{1,n}}}{\eta_1^* - \chi_1} - \frac{e^{-Z_{1,n}^* + Z_{1,n}}}{\chi_1^* - \eta_1} + \frac{e^{-Z_{1,n}^* - Z_{1,n}}}{\chi_1^* - \chi_1} \right] \\ &= \sum_{m=1, k=1}^{\infty, \infty} M_n^{[m, k]} \epsilon^{*2(m-1)} \epsilon^{2(k-1)} \end{aligned} \quad (6.2)$$

and

$$\begin{aligned} &\frac{i\beta \langle y_{1,n} | y_{1,n} \rangle}{2(\lambda_1^* - \lambda_1)} + i\beta \varphi_{1,n} \psi_{1,n} \\ &= \frac{i\beta}{4} \left[ \frac{e^{Z_{1,n}^* + Z_{1,n}}}{\eta_1^* - \eta_1} \frac{\eta_1^* + c}{\eta_1 + c} - \frac{e^{Z_{1,n}^* - Z_{1,n}}}{\eta_1^* - \chi_1} \frac{\eta_1^* + c}{\chi_1 + c} - \frac{e^{-Z_{1,n}^* + Z_{1,n}}}{\chi_1^* - \eta_1} \frac{\chi_1^* + c}{\eta_1 + c} + \frac{e^{-Z_{1,n}^* - Z_{1,n}}}{\chi_1^* - \chi_1} \frac{\chi_1^* + c}{\chi_1 + c} \right] \\ &= \sum_{m=1, k=1}^{\infty, \infty} G_n^{[m, k]} \epsilon^{*2(m-1)} \epsilon^{2(k-1)}, \end{aligned} \quad (6.3)$$

where  $\chi_1 = \eta_1(-\epsilon)$ ,

$$\left. \begin{aligned} M_n^{[m,k]} &= \sum_{i=0}^{2m-1} \sum_{j=0}^{2k-1} F^{[i,j]} S_{2k-i-1}(\mathbf{Z}_{1,n}) S_{2m-j-1}(\mathbf{Z}_{1,n}^*) \\ \text{and} \quad G_n^{[m,k]} &= \sum_{i=0}^{2m-1} \sum_{j=0}^{2k-1} F^{[i,j]} S_{2k-i-1}(\mathbf{Z}_{1,n} + \epsilon) S_{2m-j-1}(\mathbf{Z}_{1,n}^* + \epsilon) \end{aligned} \right\} \quad (6.4)$$

and  $\epsilon = (1, 0, 0, \dots)$ .

Based on the expansion equations (6.2) and (6.3), and formulae (2.9) and (2.10), we can obtain the general rogue wave solution, as follows.

**Proposition 6.2.** *The general high-order rogue wave solution for the sdCSP equation (1.11) can be represented as*

$$\left. \begin{aligned} \rho_n^{[N]} &= \frac{\gamma}{2} - \frac{2}{a} \ln_s \left( \frac{\det(M_{n+1})}{\det(M_n)} \right), \quad q_n^{[N]} = \frac{\beta}{2} \left[ \frac{\det(G_n)}{\det(M_n)} \right] e^{i\theta_n} \\ \text{and} \quad x_n^{[N]} &= \frac{\gamma}{2} an - \frac{\beta^2}{8} s - 2 \ln_s \det(M_n), \quad t = -s, \end{aligned} \right\} \quad (6.5)$$

where

$$M_n = \left( M_n^{[m,k]} \right)_{1 \leq m, k \leq N}, \quad G_n = \left( G_n^{[m,k]} \right)_{1 \leq m, k \leq N};$$

the expressions  $M_n^{[m,k]}$  and  $G_n^{[m,k]}$  are given in (6.4).

Specially, the first-order rogue wave solution can be written explicitly through formula (6.5)

$$\begin{aligned} \rho_n^{[1]} &= \frac{\gamma}{2} - \frac{2}{a} \ln_s \left( \frac{(1/4) + (Z_{n+1,R}^{[1]})^2 + (Z_{n+1,I}^{[1]} + (1/2))^2}{(1/4) + (Z_{n,R}^{[1]})^2 + (Z_{n,I}^{[1]} + (1/2))^2} \right), \\ q_n^{[1]} &= \frac{\beta}{2} \left[ 1 - \frac{1 - 2iZ_{n,R}^{[1]}}{(1/4) + (Z_{n,R}^{[1]})^2 + (Z_{n,I}^{[1]} + (1/2))^2} \right] e^{i\theta}, \\ x_n^{[1]} &= \frac{\gamma}{2} an - \frac{\beta^2}{8} s - 2 \ln_s \left( \frac{1}{4} + (Z_{n,R}^{[1]})^2 + (Z_{n,I}^{[1]} + \frac{1}{2})^2 \right), \quad t = -s, \end{aligned}$$

where

$$Z_{n,R}^{[1]} = \frac{4\beta^2 \sin^3(b/2) \cos(b/2)n}{a^2\gamma^2 + 2\beta^2 \sin^2(b)}, \quad Z_{n,I}^{[1]} = \beta \left( \frac{2a\gamma \sin^2(b/2)n}{a^2\gamma^2 + 2\beta^2 \sin^2(b)} + \frac{s}{4} \right) - \frac{1}{2}. \quad (6.6)$$

Moreover, the general second-order rogue wave solution can be represented by

$$\begin{aligned} \rho_n^{[2]} &= \frac{\gamma}{2} - \frac{2}{a} \ln_s \left( \frac{F_{1,n+1} + iF_{2,n+1}}{F_{1,n} + iF_{2,n}} \right), \quad q_n^{[2]} = \frac{\beta}{2} \left[ 1 + \frac{G_n}{F_{1,n} + iF_{2,n}} \right] e^{i\theta_n}, \\ x_n^{[2]} &= \frac{\gamma}{2} an - \frac{\beta^2}{8} s - 2 \ln_s (F_{1,n} + iF_{2,n}), \quad t = -s, \end{aligned}$$

where

$$\begin{aligned} F_{1,n} &= \left( -\frac{1}{72} \overline{Z_n^{[1]}} - \frac{1}{12} \overline{Z_n^{[3]}} + \frac{1}{36} \overline{Z_n^{[1]^3}} \right) (Z_n^{[1]})^3 + \left( \frac{1}{8} \overline{Z_n^{[1]^2}} - \frac{1}{64} \right) (Z_n^{[1]})^2 + \frac{1}{4} \overline{Z_n^{[3]}} \overline{Z_n^{[3]}} \\ &\quad + \left( -\frac{1}{72} \overline{Z_n^{[1]^3}} + \frac{1}{24} \overline{Z_n^{[3]}} + \frac{29}{288} \overline{Z_n^{[1]}} \right) Z_n^{[1]} - \frac{1}{12} \overline{Z_n^{[3]}} \overline{Z_n^{[1]^3}} - \frac{1}{64} \overline{Z_n^{[1]^2}} + \frac{1}{24} \overline{Z_n^{[1]}} \overline{Z_n^{[3]}} + \frac{1}{64}, \\ F_{2,n} &= \frac{1}{24} \overline{Z_n^{[1]^2}} \overline{Z_n^{[1]^3}} + \frac{1}{8} \overline{Z_n^{[1]^2}} \overline{Z_n^{[3]}} - \frac{1}{24} \overline{Z_n^{[1]^2}} \overline{Z_n^{[1]^3}} - \frac{1}{8} \overline{Z_n^{[1]^2}} \overline{Z_n^{[3]}} \\ &\quad + \frac{1}{12} \overline{Z_n^{[1]}} \overline{Z_n^{[1]^2}} - \frac{1}{12} \overline{Z_n^{[1]^2}} \overline{Z_n^{[1]}} + \frac{1}{32} \overline{Z_n^{[1]}} - \frac{1}{32} \overline{Z_n^{[1]}} \end{aligned}$$

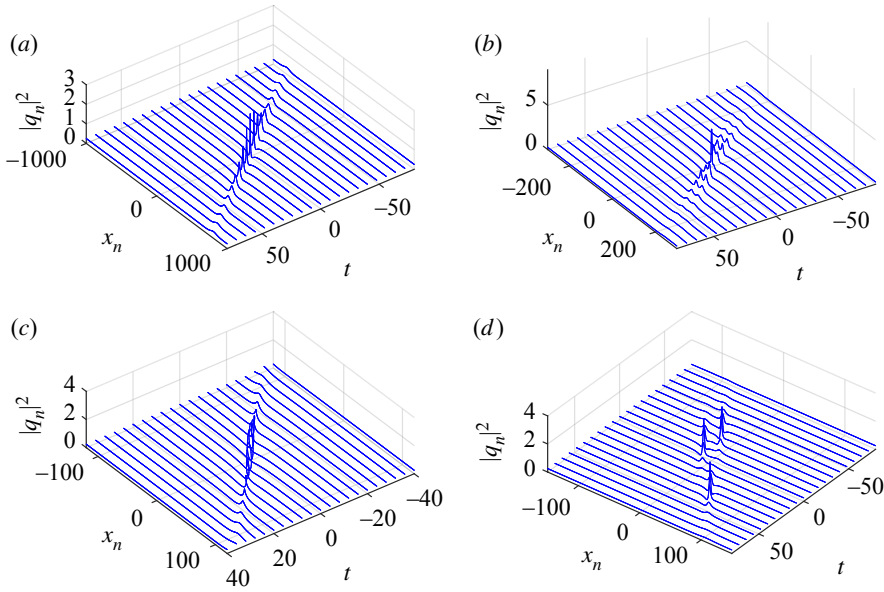


**Figure 4.** (a) Cuspon and (c) loop rogue waves and (b,d) second-order rogue waves. (Online version in colour.)

$$G_n = \frac{1}{12} \overline{iZ_n^{[1]}}^2 Z_n^{[1]3} + \left( \frac{1}{12} \overline{iZ_n^{[1]}} - \frac{1}{4} \overline{Z_n^{[1]}}^2 - \frac{1}{4} \overline{iZ_n^{[3]}} + \frac{1}{12} \overline{iZ_n^{[1]}}^3 \right) Z_n^{[1]2} - \frac{1}{12} \overline{iZ_n^{[1]}}$$

$$+ \left( \frac{1}{2} \overline{Z_n^{[3]}} - \frac{1}{6} \overline{Z_n^{[1]}}^3 - \frac{1}{6} \overline{iZ_n^{[1]}}^2 - \frac{1}{6} \overline{Z_n^{[1]}} \right) Z_n^{[1]} - \frac{1}{4} \overline{iZ_n^{[1]}}^2 Z_n^{[3]} + \frac{1}{4} \overline{iZ_n^{[3]}} - \frac{1}{12} \overline{iZ_n^{[1]}}^3,$$

where  $Z_n^{[1]} = Z_{n,R}^{[1]} + iZ_{n,I}^{[1]}$ , the symbol overbar denotes the complex conjugation and

$$Z_n^{[3]} = \frac{(2/3)i\beta \sin^2((1/2)b) \left( 2a\beta\gamma \sin(b) + ia^2\gamma^2 + 8i\beta^2 \sin^2((1/2)b) \right) n}{2\beta a^2\gamma^2 \sin(b) - \beta^3 \sin^3(b) - ia^3\gamma^3 + 3ia\beta^2\gamma \sin^2(b)} \frac{n}{2} - \frac{i\beta s}{24} + (e_1 + if_1).$$

As for the breather solution, the rogue wave solution may become singular if  $\rho_n^{[1]} \approx \frac{\partial}{\partial n} x_n^{[1]} \leq 0$  as  $a \rightarrow 0$ . The dynamics of a regular rogue wave is similar to that of the regular rogue wave in the CSP equation. The cuspon-type rogue wave is shown in figure 4a with parameters  $a = 1/10$ ,  $b = \pi/2$ ,  $\beta = 1$ ,  $\gamma = 10\sqrt{79}$ , while the loop-type rogue wave is shown in figure 4c with parameters  $a = 1/10$ ,  $b = \pi/2$ ,  $\beta = 1$ ,  $\gamma = 50$ .

For the second-order regular rogue waves, we firstly choose the parameters  $a = 2$ ,  $b = \pi/2$ ,  $\beta = 1$ ,  $\gamma = 5/2$ ,  $e_1 = f_1 = 0$ , then the standard second-order rogue waves are shown in figure 4b. To exhibit the other dynamics for the second-order regular rogue waves, we choose the parameters  $a = 2$ ,  $b = \pi/2$ ,  $\beta = 1$ ,  $\gamma = 3/2$ ,  $e_1 = 10$ ,  $f_1 = 0$ . It can be seen that the temporal-spatial distribution exhibits a triangular shape, as shown in figure 4d.

We remark here that, since the higher-order rogue wave solution is obtained from the multi-breather solution to the sdCSP equation, which converges to its counterpart in the continuous CSP equation, the high-order rogue wave solution for the sdCSP equation should converge to the one for the CSP equation in the continuous limit.

## 7. Conclusion and discussions

In the present paper, we firstly derive the generalized DT for the sdCSP equation (1.11) with the aid of the discrete hodograph transformation. Based on formulae derived from the generalized DT, we then construct the multi-bright soliton solution for the focusing CSP equation with zero

boundary condition, whose results have been obtained by Hirota's bilinear method [58,59]. On the other hand, starting from the non-zero seed solution, we further construct the multi-dark soliton solution for the defocusing sdCSP equation and multi-breather solution for the focusing sdCSP equation. Moreover, based on the multi-breather solution, we derive the general high-order rogue wave solution. As far as we know, the multi-dark, multi-breather and general high-order rogue wave solutions are obtained for the first time in the literature for this new sdCSP equation.

Over the past half-century, the single most important driving factor in the advance of optics and photonics has been the impact of the laser in providing coherent electromagnetic waves over an increasingly wide spectral range. Theoretical and experimental studies at the femtosecond level not only permitted dramatic new insights into the dynamics of materials and non-equilibrium properties but also allowed the development of the fibre-optic communication backbone of the modern economy. As an analogue of the AL lattice in the ultra-short regime, it is expected that the solutions obtained will help scientists to better understand the coherent dynamics of nonlinear ultra-short pulses.

It is found that the condition  $\rho_n > 0$  is required to keep the non-singularity or the smooth property of the solution. Otherwise, the cusp-type solution occurs if  $\rho_n = 0$  and the loop-type soliton appears if  $\rho_n < 0$  for either bright, dark, breather or rogue wave solutions. The occurrence of the singularity of the solution is different from that of the AL lattice equation, which is a new finding in this semi-discrete model. We have illustrated, in the present paper, cuspon-type and loop-type bright, dark, breather and rogue wave solutions to the sdCSP equation.

In [69], we have constructed various solutions to the NLS equation with an elliptic function boundary condition; a natural extension would be the study of dark breather solutions to the CSP equation and its semi-discrete analogue with an elliptic function boundary. Moreover, a robust IST method was recently proposed for the NLS equation by appropriately setting up and solving the Riemann–Hilbert problem [70,71]. It is imperative to study the IST and Riemann–Hilbert problem for the sdCSP equation.

In conclusion, we should point out that the following coupled sdCSP equation:

$$\left. \begin{aligned} \frac{d}{dt}(q_{1,n+1} - q_{1,n}) &= \frac{1}{2}(x_{n+1} - x_n)(q_{1,n+1} + q_{1,n}), \\ \frac{d}{dt}(q_{2,n+1} - q_{2,n}) &= \frac{1}{2}(x_{n+1} - x_n)(q_{2,n+1} + q_{2,n}) \end{aligned} \right\} \quad (7.1)$$

and

$$\frac{d}{dt}(x_{n+1} - x_n) + \frac{1}{2} \sum_{j=1}^2 \sigma_j (|q_{j,n+1}|^2 - |q_{j,n}|^2) = 0$$

has been shown to be integrable [59]. Beside the multi-bright soliton solution implied in [59], how about its general initial value problem and other types of soliton solutions?

The method provided in this paper is also useful for the coupled sdCSP equation. We expect to obtain and report the results in the near future. Finally, the semi-discrete equations obtained can be used as superior numerical schemes: the so-called self-adaptive moving mesh schemes for the CSP and coupled CSP equations.

**Data accessibility.** This article has no additional data.

**Authors' contributions.** B.-F.F. and Z.Z. formulated the problem. L.L. and Z.Z. constructed the generalized DT. All authors contributed to the development of various solutions and to writing the manuscript. All authors agree to be accountable for all aspects of the work.

**Competing interests.** We declare we have no competing interests.

**Funding.** The work of B.-F.F. is supported by the NSF (grant no. DMS-1715991), the US Department of Defense (DoD) and the US Air Force for Scientific Research (AFOSR) (grant no. W911NF2010276). The work of L.L. is supported by the National Natural Science Foundation of China (grant no. 11771151) and by the Guangzhou Science and Technology Program (grant no. 201904010362). The work of Z.Z. is supported by the National Natural Science Foundation of China (grant nos. 12071286 and 11671255) and by the Ministry of Economy and Competitiveness of Spain under contract MTM2016-80276-P (AEI/FEDER, EU).

**Acknowledgements.** B.-F.F. acknowledges the useful discussions with Y. Ohta and K. Maruno.

## References

- Pedersen S, Herek JL, Zewail AH. 1994 The validity of the diradical hypothesis: direct femtosecond studies of the transition-state structures. *Science* **266**, 1359–1364. (doi:10.1126/science.266.5189.1359)
- Donna S, Gerard M. 1985 Compression of amplified chirped optical pulses. *Optics Commun.* **56**, 219–221. (doi:10.1016/0030-4018(85)90120-8)
- Agrawal GP. 1995 *Nonlinear fiber optics*. New York, NY: Academic Press.
- Hasegawa A, Kodama Y. 1995 *Solitons in optical communications*. Oxford, UK: Clarendon.
- Kivshar YS, Agrawal GP. 2003 *Optical solitons: from fibers to photonic crystals*. San Diego, CA: Academic Press.
- Hasegawa A, Tappert F. 1973 Transmission of stationary nonlinear optical pulses in dispersive dielectric fibers I. Anomalous dispersion. *Appl. Phys. Lett.* **23**, 142. (doi:10.1063/1.1654836)
- Hasegawa A, Tappert F. 1973 Transmission of stationary nonlinear optical pulses in dispersive dielectric fibers II. Normal dispersion. *Appl. Phys. Lett.* **23**, 171. (doi:10.1063/1.1654847)
- Ablowitz MJ, Clarkson PA. 1991 *Solitons, nonlinear evolution equations and inverse scattering*. London Mathematical Society Lecture Notes Series, vol. 149. Cambridge, UK: Cambridge University Press.
- Ablowitz MJ, Prinari B, Trubatch AD. 2004 *Discrete and continuous nonlinear Schrödinger systems*. Cambridge, UK: Cambridge University Press.
- Dalfovo F, Giorgini S, Stringari LP. 1999 Theory of Bose-Einstein condensation in trapped gases. *Rev. Mod. Phys.* **71**, 463–512. (doi:10.1103/RevModPhys.71.463)
- Benney DJ, Newell AC. 1967 The propagation of nonlinear wave envelopes. *Stud. Appl. Math.* **46**, 133–139. (doi:10.1002/sapm1967461133)
- Zakharov VE. 1972 Collapse of Langmuir waves. *Sov. Phys. JETP* **35**, 908–914.
- Zakharov VE, Shabat AB. 1972 Exact theory of two-dimensional self-focusing and one-dimensional self-modulations of waves in nonlinear media. *Sov. Phys. JETP* **34**, 62–69.
- Krokel D, Halas NJ, Giuliani G, Grischkowsky D. 1988 Dark-pulse propagation in optical fibers. *Phys. Rev. Lett.* **60**, 29. (doi:10.1103/PhysRevLett.60.29)
- Weiner AM, Heritage JP, Hawkins RJ, Thurston RN, Kirschner EM, Leaird DE, Tomlinson WJ. 1988 Experimental observation of the fundamental dark soliton in optical fibers. *Phys. Rev. Lett.* **61**, 2445. (doi:10.1103/PhysRevLett.61.2445)
- Kibler B, Fatome J, Finot C, Millot G, Dias F, Genty G, Akhmediev N, Dudley JM. 2010 The Peregrine soliton in nonlinear fibre optics. *Nat. Phys.* **6**, 790–795. (doi:10.1038/nphys1740)
- Hirota R. 1973 Exact envelope-soliton solutions of a nonlinear wave equation. *J. Math. Phys.* **14**, 805–809. (doi:10.1063/1.1666399)
- Sasa N, Satsuma J. 1991 New-type soliton solution for a higher-order nonlinear Schrödinger equation. *J. Phys. Soc. Jpn* **60**, 409–417. (doi:10.1143/JPSJ.60.409)
- Rothenberg JE. 1992 Space-time focusing: breakdown of the slowly varying envelope approximation in the self-focusing of femtosecond pulses. *Opt. Lett.* **17**, 1340–1342. (doi:10.1364/OL.17.001340)
- Skobelev SA, Kartashov DV, Kim AV. 2007 Few-optical-cycle solitons and pulse self-compression in a Kerr medium. *Phys. Rev. Lett.* **99**, 203902. (doi:10.1103/PhysRevLett.99.203902)
- Kim AV, Skobelev SA, Anderson D, Hansson T, Lisak M. 2008 Extreme nonlinear optics in a Kerr medium: exact soliton solutions for a few cycles. *Phys. Rev. A* **77**, 043823. (doi:10.1103/PhysRevA.77.043823)
- Amiranashvili S, Bandelow U, Akhmediev N. 2013 Few-cycle optical solitary waves in nonlinear dispersive media. *Phys. Rev. A* **87**, 013805. (doi:10.1103/PhysRevA.87.013805)
- Schäfer T, Wayne CE. 2004 Propagation of ultrashort optical pulses in cubic nonlinear media. *Physica D* **196**, 90–105. (doi:10.1016/j.physd.2004.04.007)
- Sakovich A, Sakovich S. 2005 The short pulse equation is integrable. *J. Phys. Soc. Jpn* **74**, 239–241. (doi:10.1143/JPSJ.74.239)
- Matsuno Y. 2008 Periodic solutions of the short pulse model equation. *J. Math. Phys.* **49**, 073508. (doi:10.1063/1.2951891)
- Liu Y, Pelinovsky D, Sakovich A. 2009 Wave breaking in the short-pulse equation. *Dynam. Part. Differ. Equ.* **6**, 291–310. (doi:10.4310/DPDE.2009.v6.n4.a1)
- Feng B-F, Maruno K, Ohta Y. 2010 Integrable discretizations of the short pulse equation. *J. Phys. A* **43**, 085203. (doi:10.1088/1751-8113/43/8/085203)

28. Feng B-F, Inoguchi J, Kajiwara K, Maruno K, Ohta Y. 2011 Discrete integrable systems and hodograph transformations arising from motions of discrete plane curves. *J. Phys. A* **44**, 395201. (doi:10.1088/1751-8113/44/39/395201)
29. Feng B-F. 2015 Complex short pulse and coupled complex short pulse equations. *Physica D* **297**, 62–75. (doi:10.1016/j.physd.2014.12.002)
30. Feng B-F, Ling L, Zhu Z. 2016 A defocusing complex short pulse equation and its multi-dark soliton solution by Darboux transformation. *Phys. Rev. E* **93**, 052227. (doi:10.1103/PhysRevE.93.052227)
31. Shen S, Feng B-F, Ohta Y. 2016 From the real and complex coupled dispersionless equations to the real and complex short pulse equations. *Stud. Appl. Math.* **136**, 64–88. (doi:10.1111/sapm.12092)
32. Ling L, Feng B-F, Zhu Z. 2016 Multi-soliton, multi-breather and higher order rogue wave solutions to the complex short pulse equation. *Physica D* **327**, 13–29. (doi:10.1016/j.physd.2016.03.012)
33. van der Mee C. 2020 Complex short-pulse solutions by gauge transformation. *J. Geom. Phys.* **148**, 103539. (doi:10.1016/j.geomphys.2019.103539)
34. Prinari B, Trubatch AD, Feng B-F. 2020 Inverse scattering transform for the complex short-pulse equation by a Riemann–Hilbert approach. *Eur. Phys. J. Plus* **135**, 717. (doi:10.1140/epjp/s13360-020-00714-z)
35. Xu J, Fan E. 2020 Long-time asymptotic behavior for the complex short pulse equation. *J. Differ. Equ.* **269**, 10322–10349. (doi:10.1016/j.jde.2020.07.009)
36. Feng B-F, Maruno K, Ohta Y. 2016 Geometric formulation and multi-dark soliton solution to the defocusing complex short pulse equation. *Stud. Appl. Math.* **138**, 343–367. (doi:10.1111/sapm.12159)
37. Li B-Q, Ma Y-L. 2017 Periodic solutions and solitons to two complex short pulse (CSP) equations in optical fiber. *Optik* **144**, 149–155. (doi:10.1016/j.ijleo.2017.06.114)
38. Ablowitz MJ, Feng B-F, Luo X-D, Musslimani ZH. 2018 Reverse space-time sine/sinh-Gordon equations with nonzero boundary conditions. *Stud. Appl. Math.* **141**, 267–307. (doi:10.1111/sapm.12222)
39. Kamchatnov AM. 2000 *Nonlinear periodic waves and their modulations*. Hong Kong: World Scientific Press.
40. Hietarinta J, Joshi N, Nihoff FW. 2016 *Discrete systems and integrability*. Cambridge, UK: Cambridge University Press.
41. Hirota R. 1977 Nonlinear partial difference equations. I. A difference analogue of the Korteweg-de Vries equation. *J. Phys. Soc. Jpn* **43**, 1424. (doi:10.1143/JPSJ.43.1424)
42. Ablowitz MJ, Ladik JF. 1975 Nonlinear differential-difference equations. *J. Math. Phys.* **16**, 598–603. (doi:10.1063/1.522558)
43. Ablowitz MJ, Ladik JF. 1976 Nonlinear differential-difference equations and Fourier analysis. *J. Math. Phys.* **17**, 1011–1018. (doi:10.1063/1.523009)
44. Tsujimoto S. 2000 Discretization of integrable system. In *Applied integrable systems* (ed. Y Nakamura), ch. 1. Tokyo, Japan: Shokabo. [In Japanese.]
45. Narita K. 1990 Soliton solution for discrete Hirota equation. *J. Phys. Soc. Jpn* **59**, 3528–3530. (doi:10.1143/JPSJ.59.3528)
46. Maruno K, Ohta Y. 2006 Casorati determinant form of dark soliton solutions of the discrete nonlinear Schrödinger equation. *J. Phys. Soc. Jpn* **75**, 054002. (doi:10.1143/JPSJ.75.054002)
47. Vekslerchik VE, Konotop VV. 1992 Discrete nonlinear Schrödinger equation under non-vanishing boundary conditions. *Inv. Prob.* **8**, 889–909. (doi:10.1088/0266-5611/8/6/007)
48. Ablowitz MJ, Biondini G, Prinari B. 2007 Inverse scattering transform for the integrable discrete nonlinear Schrödinger equation with non-vanishing boundary conditions. *Inv. Prob.* **23**, 1711–1758. (doi:10.1088/0266-5611/23/4/021)
49. Van Der Mee C. 2015 Inverse scattering transform for the discrete focusing nonlinear Schrödinger equation with non-vanishing boundary conditions. *J. Nonlinear Math. Phys.* **22**, 233–264. (doi:10.1080/14029251.2015.1023583)
50. Prinari B, Vitale F. 2015 Inverse scattering transform for the focusing Ablowitz-Ladik system with nonzero boundary conditions. *Stud. Appl. Math.* **137**, 28–52. (doi:10.1111/sapm.12103)
51. Ankiewicz A, Akhmediev N, Soto-Crespo JM. 2010 Discrete rogue waves of the Ablowitz-Ladik and Hirota equations. *Phys. Rev. E* **82**, 026602. (doi:10.1103/PhysRevE.82.026602)

52. Ankiewicz A, Devine N, Unal M, Chowdury A, Akhmediev N. 2013 Rogue waves and other solutions of single and coupled Ablowitz-Ladik and nonlinear Schrödinger equations. *J. Optics* **15**, 064008. (doi:10.1088/2040-8978/15/6/064008)
53. Ohta Y, Yang J. 2014 General rogue waves in the focusing and defocusing Ablowitz-Ladik equations. *J. Phys. A: Math. Theor.* **47**, 255201. (doi:10.1088/1751-8113/47/25/255201)
54. Doliwa A, Santini PM. 1995 Integrable dynamics of a discrete curve and the Ablowitz-Ladik hierarchy. *J. Math. Phys.* **36**, 1259–1273. (doi:10.1063/1.531119)
55. Takeno S, Hori K. 1990 A propagating self-localized mode in a one-dimensional lattice with quartic anharmonicity. *J. Phys. Soc. Jpn* **59**, 3037–3040. (doi:10.1143/JPSJ.59.3037)
56. Kenkre VM, Campbell DK. 1986 Self-trapping on a dimer: time-dependent solutions of a discrete nonlinear Schrödinger equation. *Phys. Rev. B* **34**, 495–4961. (doi:10.1103/PhysRevB.34.4959)
57. Papanicoulau N. 1987 Complete integrability for a discrete Heisenberg chain. *J. Phys. A: Math. Gen.* **20**, 3637–3652. (doi:10.1088/0305-4470/20/12/018)
58. Feng B-F, Maruno K, Ohta Y. 2014 Self-adaptive moving mesh schemes for short pulse type equations and their Lax pairs. *Pacific J. Math. Industry* **6**, 1–14. (doi:10.1186/s40736-014-0001-1)
59. Feng B-F, Maruno K, Ohta Y. 2015 Integrable discretization of a multi-component short pulse equation. *J. Math. Phys.* **56**, 043502. (doi:10.1063/1.4916895)
60. Terng CL, Uhlenbeck K. 2000 Bäcklund transformations and loop group actions. *Commun. Pure Appl. Math.* **53**, 1–75. (doi:10.1002/(SICI)1097-0312(200001)53:1<1::AID-CPA1>3.0.CO;2-U)
61. Matveev VB, Salle MA. 1991 *Darboux transformations and solitons*. Berlin, Germany: Springer.
62. Guo B, Ling L, Liu QP. 2012 Nonlinear Schrödinger equation: generalized Darboux transformation and rogue wave solutions. *Phys. Rev. E* **85**, 026607. (doi:10.1103/PhysRevE.85.026607)
63. Xu T, Lan S, Li M, Li L-L, Zhang G-W. 2019 Mixed soliton solutions of the defocusing nonlocal nonlinear Schrödinger equation. *Physica D* **390**, 47–61. (doi:10.1016/j.physd.2018.11.001)
64. Wajahat H, Riaz A, ul Hassan M. 2017 Darboux transformation of a semi-discrete coupled dispersionless integrable system. *Commun. Nonlinear Sci. Numer. Simulat.* **48**, 387–397. (doi:10.1016/j.cnsns.2017.01.011)
65. Ling L, Zhao LC, Guo B. 2015 Darboux transformation and multi-dark soliton for N-component nonlinear Schrödinger equations. *Nonlinearity* **28**, 3243. (doi:10.1088/0951-7715/28/9/3243)
66. Degasperis A, Lombardo S. 2007 Multicomponent integrable wave equations: I. Darboux-dressing transformation. *J. Phys. A: Math. Theor.* **40**, 961. (doi:10.1088/1751-8113/40/5/007)
67. Baronio F, Conforti M, Degasperis A, Lombardo S, Onorato M, Wabnitz S. 2014 Vector rogue waves and baseband modulation instability in the defocusing regime. *Phys. Rev. Lett.* **113**, 034101. (doi:10.1103/PhysRevLett.113.034101)
68. Degasperis A, Lombardo S, Sommacal M. 2019 Rogue wave type solutions and spectra of coupled nonlinear Schrödinger equations. *Fluids* **4**, 57. (doi:10.3390/fluids4010057)
69. Feng B-F, Ling L, Takahashi D. 2020 Multi-breather and high order rogue waves on the elliptic function background. *Stud. Appl. Math.* **142**, 46–101. (doi:10.1111/sapm.12287)
70. Bilman D, Miller PD. 2019 A robust inverse scattering transform for the focusing nonlinear Schrödinger equation. *Commun. Pure Appl. Math.* **72**, 1722–1805. (doi:10.1002/cpa.21819)
71. Bilman D, Ling L, Miller PD. 2020 Extreme superposition: rogue waves of infinite order and the Painlevé-III hierarchy. *Duke Math. J.* **169**, 671–760. (doi:10.1215/00127094-2019-0066)